Supporting Information

2D/2D Mo_2CT_x/g-C_3N_4 with a strong coupling interface via one-step NH_4Cl-assisted calcination for enhanced photocatalytic hydrogen production

Haiting Zou[a], Miaomiao Pan[a], Ping Wang[a, *], Xuefei Wang[a], Feng Chen [a], Huogen Yu[a,b, *]

[a]School of Chemistry, Chemical Engineering and Life Sciences, Wuhan University of Technology, Wuhan 430070,PR China

[b]Laboratory of Solar Fuel, Faculty of Materials Science and Chemistry, China University of Geosciences, Wuhan, 430074, PR China

*Corresponding authors. Tel: +86(27)87749379;

E-mail: wangping0904@whut.edu.cn (Ping Wang);

huogenyu@163.com (Huogen Yu)

SI Experimental

SI-1 Materials

Mo_2Ga_2C, guanidine hydrochloride (CH_6ClN_3), ammonium chloride (NH_4Cl), ammonium fluoride (NH_4F), hydrochloric acid (HCl), lactic acid ($CH_3CH(OH)COOH$) and sodium sulfide (Na_2SO_4) are used as analytical fluids.

SI-2 Characterization

XRD patterns of photocatalysts were recorded using a rotation anode high-power X-ray diffractometer (Rigaku Kα III). The Fourier transform infrared (FTIR) spectra were recorded on a spectrometer (Nicolet6700). The SEM and TEM results were revealed by JSM-7500F and FEI Talos F200S, respectively. UV–vis spectra were obtained by a UV-2450 spectrophotometer. The surface chemical composition was analyzed on a scanning X-ray microprobe (ESCALAB 250Xi).

SI-3 Photocatalytic H_2 production activity measurement

To test the photocatalytic performance, 50 mg of the synthesized photocatalyst was dispersed into 80 mL of lactic acid aqueous and stirred for 30 minutes. Then the air in the three-neck flask was drained by degassing with nitrogen for 15 minutes. Subsequently irradiated by an LED lamp (3-W, 420 nm, Shenzhen, China). Then 40 μL gas was taken every 30 minutes by syringe to the gas chromatograph for testing (GC-2014C, Shimadzu Corporation). Herein, the gas chromatograph uses a TCD detector and 5 A molecular sieve column, with N_2 as the carrier gas. A photocatalytic H_2 production test is completed within 2 hours. After finishing 1st run, the above suspension (without filtration, washing, and drying) was re-bubbled with N_2 for 30 min

to remove the generated H_2 and was reused for the next H_2-evolution test. Subsequently, the 2nd, 3rd, and 4th runs were coherently tested under the same process.

The apparent quantum efficiency (AQE) of Mo_2CT_x/g-C_3N_4 and Mo_2CT_x-g-C_3N_4 photocatalysts is calculated via the following equation:

$$\begin{aligned} \mathrm{AQE}(\%) &= \frac{\text{number of reacted electrons}}{\text{number of incident photons}} \times 100 \\ &= \frac{\text{number of evolved } H_2 \text{ molecules} \times 2}{\text{number of incident photons}} \times 100 \end{aligned} \quad \text{(S1)}$$

The average power of the UV-light (four 3-W 420 nm) was 50 mW/cm^2.

SI-4 Photoelectrochemical measurements

Electrochemical analyzer (CHI 660 E, China) was used to test the photoelectric chemical curve (PEC) of the sample. The synthesized sample was used as the working electrode, the standard Ag/AgCl electrode as the reference electrode, and the Pt electrode was used to make a three-electrode device. The working electrodes were prepared on FTO conductive glass. First, 10 mg sample was dispersed in 2.5 ml ethanol solution and ultrasonic for 15 minutes to form a dispersion solution. Second, 0.5 ml dispersed droplets were added to 0.5 ml Nafion-ethanol mixed solution (the ratio of ethanol to Nafion membrane solution was 4:1), and ultrasound was continued for 15 minutes. Third, 30 μL dispersion was removed and added to the FTO conductive glass and rotated for 15 s at a rotational speed of 700 r min^{-1}, repeated 10 times. Last, FTO conductive glass with uniformly loaded sample was placed in the oven to dry. Linear sweep voltammetry (LSV) curves were obtained in the potential range of -1.0 to -1.6 V at a sweep rate of 10 mV s^{-1}. Transient photocurrent responses with time (i-t curve) were recorded during the periodic ON/OFF lighting cycle under a 3-W LED lamp (420

nm) and 0.5 V bias, and the electrochemical impedance spectroscopy (EIS) tests were performed at an open circuit voltage, at the frequency range of 0.01-105 hz with an ac amplitude of 10 mV under the open-circuit voltage.

SI-5. Density functional theory calculation

The calculations were carried out by utilizing Vienna Ab-initio simulation package (VASP) [1-3]. The exchange-correlation effects were revealed by generalized gradient approximation (GGA) and Purdewy-Burke-Ernzerhof(PBE) functional. The g-C_3N_4 (002) structure was built with 16 N atoms and 12 C atoms. The Mo_2CT_x model was constructed by removing Ga atoms from the Mo_2Ga_2C (001) model and constructing a (3×3×1) supercell containing 36 Mo atoms and 18 C atoms (adding 15 A vacuum). The cutoff energy and Monkhorst-Pack k-point mesh were set as 450 eV and 3 × 3 × 1, respectively. The convergence threshold d for total energy converged within 10^{-5} eV/atom and 0.01 eV·$Å^{-1}$ for force. The partial occupancies were determined using the Gaussian smearing scheme with a smearing width of 0.2 eV. To eliminate interactions between periodic structures, a vacuum of 15 Å was added. The Gibbs free energy of H atom adsorption (ΔG_{H*}) was defined as following the equation S2:

$$\Delta G_{H*} = \Delta E_{H*} + \Delta E_{ZPE} - T\Delta S_H \quad \text{(S2)}$$

where ΔE_{H*}, ΔE_{ZPE}, and $T\Delta S_H$ are the differential hydrogen ΔE_{H*} adsorption energy, the change in zero-point energy and entropy between the adsorbed hydrogen and molecular hydrogen in the gas phase, respectively, and T is the temperature. By default the entropy of H_2 gas at 298 K is 130 J·mol^{-1}·K^{-1}, so the term $T\Delta S_H$ was calculated to be -0.20 eV.

References

1. H. Long, P. Wang, X. Wang, F. Chen, H. Yu, *Appl. Sur. Sci.* 2022, **604**, 154457.

2. D. Gao, H. Long, X. Wang, J. Yu, H. Yu, *Adv. Funct. Mater.*, 2022, **34**, 210847.

3. W. Zhong, B. Zhao, X. Wang, P. Wang, H. Yu, *ACS Catal.*, 2023, **13**, 749-756.

Figure captions

Fig. S1. FESEM images and AFM of Mo_2CT_x (A, B) and $Mo_2CT_x(NH_4Cl)$ (C, D).

Fig. S2. The photocatalytic H_2-evolution activity of $Mo_2CT_x/g\text{-}C_3N_4$ (A) at different pH values in ethanol solution (25 vol%) and (B) in lactic acid (10 vol%, pH = ca. 3), ethanol (25 vol%, pH = ca. 7), and TEOA (10 vol%, pH = ca. 9) solution.

Fig. S3. (A) The XRD patterns and (B) UV-vis spectra of $Mo_2CT_x/g\text{-}C_3N_4$ before (a) and after (b) irradiation.

Fig. S4. XPS survey spectra of $g\text{-}C_3N_4$, $Mo_2CT_x\text{-}g\text{-}C_3N_4$, and $Mo_2CT_x/g\text{-}C_3N_4$.

Table S1. Raw material ratios (the yield of g-C_3N_4 from CH_6ClN_3 is approximately 26%).

Sample	NH_4Cl (g)	CH_6ClN_3 (g)	Mo_2CT_x (mg)
g-C_3N_4	2	1	-
Mo_2CT_x/g-C_3N_4(3%)	2	1	7.8
Mo_2CT_x/g-C_3N_4(10%)	2	1	26
Mo_2CT_x/g-C_3N_4(15%)	2	1	39
Mo_2CT_x/g-C_3N_4(20%)	2	1	52

Table S2. The H_2-evolution performance and apparent quantum efficiency (AQE) of various samples.

Sample	H_2-production activity (μmol h^{-1} g^{-1})	AQE (%)
g-C_3N_4	5	0.16
Mo_2CT_x/g-C_3N_4(3%)	48	1.49
Mo_2CT_x/g-C_3N_4(10%)	96	2.98
Mo_2CT_x/g-C_3N_4(15%)	125	3.88
Mo_2CT_x/g-C_3N_4(20%)	76	2.36
Mo_2CT_x-g-C_3N_4(15%)	7	0.22

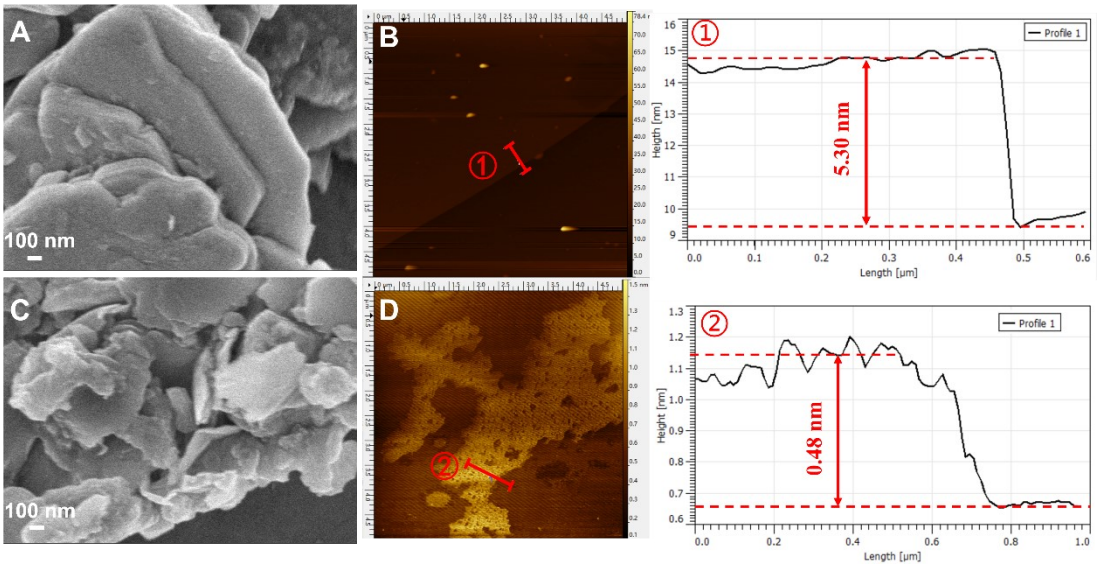

Fig. S1. FESEM images and AFM of Mo_2CT_x (A, B) and $Mo_2CT_x(NH_4Cl)$ (C, D)

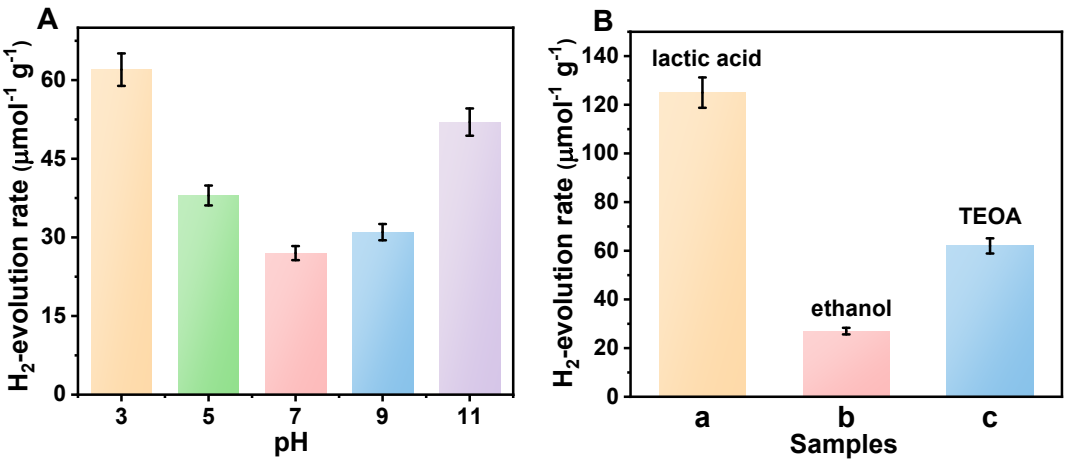

Fig. S2. The photocatalytic H_2-evolution activity of Mo_2CT_x/g-C_3N_4 (A) at different pH values in ethanol solution (25 vol%) and (B) in lactic acid (10 vol%, pH = ca. 3), ethanol (25 vol%, pH = ca. 7), and TEOA (10 vol%, pH = ca. 9) solution.

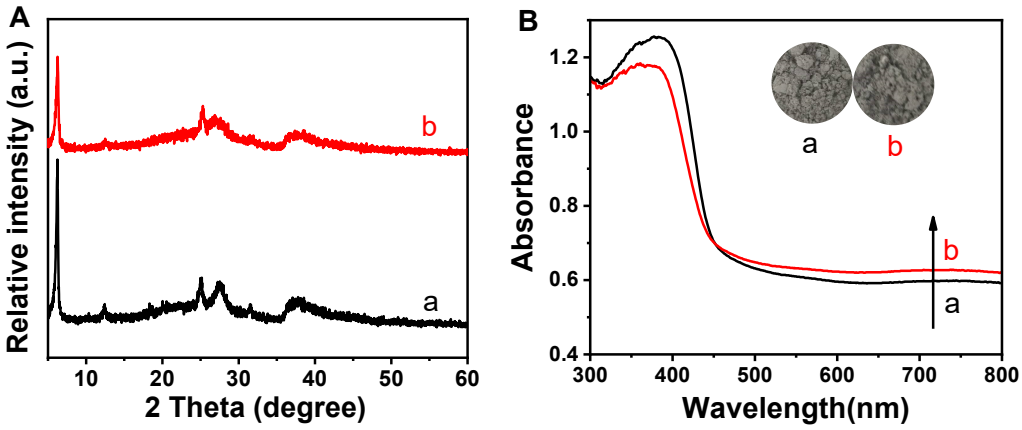

Fig. S3. (A) XRD patterns and (B) UV-vis spectra of Mo_2CT_x/g-C_3N_4(15%) before (a) and after (b) irradiation.

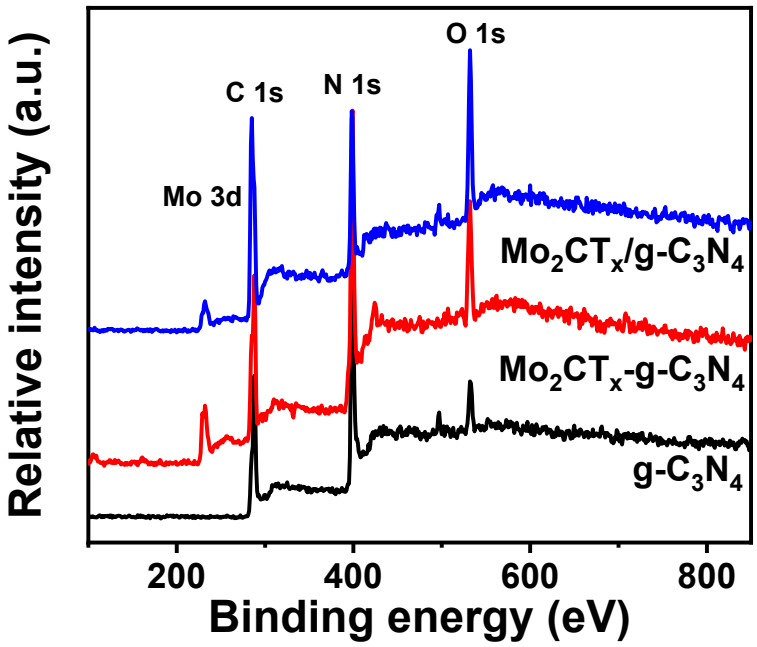

Fig. S4. XPS survey spectra of g-C_3N_4, Mo_2CT_x-g-C_3N_4, and Mo_2CT_x/g-C_3N_4.